



Vertical Silicon Nanowire Field Effect Transistors with Nanoscale Gate-All-Around

Yousseuf Guerfi, Guilhem Larrieu

► To cite this version:

Yousseuf Guerfi, Guilhem Larrieu. Vertical Silicon Nanowire Field Effect Transistors with Nanoscale Gate-All-Around. Nanoscale Research Letters, 2016, 11, pp.210. 10.1186/s11671-016-1396-7 . hal-01942311

HAL Id: hal-01942311

<https://laas.hal.science/hal-01942311>

Submitted on 26 Jun 2019

HAL is a multi-disciplinary open access archive for the deposit and dissemination of scientific research documents, whether they are published or not. The documents may come from teaching and research institutions in France or abroad, or from public or private research centers.

L'archive ouverte pluridisciplinaire **HAL**, est destinée au dépôt et à la diffusion de documents scientifiques de niveau recherche, publiés ou non, émanant des établissements d'enseignement et de recherche français ou étrangers, des laboratoires publics ou privés.

NANO EXPRESS

Open Access



Vertical Silicon Nanowire Field Effect Transistors with Nanoscale Gate-All-Around

Youssef Guerfi and Guilhem Larrieu*

Abstract

Nanowires are considered building blocks for the ultimate scaling of MOS transistors, capable of pushing devices until the most extreme boundaries of miniaturization thanks to their physical and geometrical properties. In particular, nanowires' suitability for forming a gate-all-around (GAA) configuration confers to the device an optimum electrostatic control of the gate over the conduction channel and then a better immunity against the short channel effects (SCE). In this letter, a large-scale process of GAA vertical silicon nanowire (VNW) MOSFETs is presented. A top-down approach is adopted for the realization of VNWs with an optimum reproducibility followed by thin layer engineering at nanoscale. Good overall electrical performances were obtained, with excellent electrostatic behavior (a subthreshold slope (SS) of 95 mV/dec and a drain induced barrier lowering (DIBL) of 25 mV/V) for a 15-nm gate length. Finally, a first demonstration of dual integration of n-type and p-type VNW transistors for the realization of CMOS inverter is proposed.

Background

The continuous demand of high-performance and low-power devices necessitates integration density enhancement, which pushes the CMOS technology to the ultimate nanoscale size dimension. Nanowire (NW) MOSFETs [1–5] are considered the most promising candidates to pursue the downscaling of MOS transistors, outperforming of triple gate FinFET architectures for sub-7-nm technology node. Indeed, nanowire architecture is more suitable for gate-all-around configuration to preserve the device immunity against the short channel effects (SCE) at such scaled dimensions [6, 7]. This architecture is speculated to bring CMOS scaling to the end of the transistor roadmap [8]. The NW manufacturing method could be divided into two main approaches: bottom-up (BU) and top-down (TD). The first one suffers from process complexity [9] and metallic contamination issues since metallic nanoparticles are used as a catalyst. In contrast, the TD approach, using conventional microfabrication tools, is more suitable for nanoelectronic applications. It offers perfect control over dimensions, localization, and orientation which leads to highly efficient NW MOSFET devices [10–12]. The integration of the NW-based MOSFETs can be horizontal or vertical. From

design analysis, vertical integration could give a better integration density of 50 % over the horizontal one [13, 14]. Moreover, gate-all-around definition in vertical configuration, even at nanoscale, is not defined by high-resolution lithography but simply by the thickness of deposited gate material [15, 16]. In this letter, we present a large-scale process for manufacturing of GAA vertical silicon nanowire (VNW) MOSFETs with a 15-nm gate length. The electrical performances will be discussed, in particular the influence of nanowire diameter on the device operation. Finally, a proof of concept for a CMOS inverter will be presented.

Methods

In Fig. 1, the fabrication steps of a Si VNW MOSFET are presented. After the realization of the VNWs (Fig. 1a), an SiO₂ layer acting as gate oxide is grown and remained only on the sidewalls of the nanowires forming a Si–SiO₂ core–shell structure (Fig. 1b). Then, the realization of silicided contacts at both sides of the Si VNWs for the realization of low resistive source/drain contacts is shown (Fig. 1c). The next step consists of the realization of the source to gate insulating spacer (Fig. 1d), followed by the formation of the metallic gate-all-around (Fig. 1e) and by the gate-drain insulating spacer (Fig. 1f). Finally, the electrical contacts are defined on top of the architecture and are connected to the bottom and gate contact extensions using vias through the insulation layers (Fig. 1g).

* Correspondence: glarrieu@laas.fr

LAAS-CNRS, Université de Toulouse, CNRS, 7 av. Roche, Toulouse 31077, France

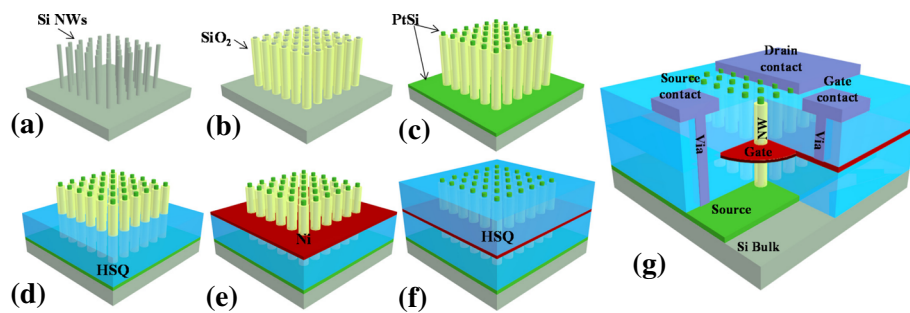


Fig. 1 Schematic 3D illustrations of the process steps of Si VNW GAA MOSFET. **a** Si VNW network patterning. **b** Gate oxide definition. **c** Metallic S/D contacts. **d** Gate to source isolating spacer. **e** Gate-all-around definition. **f** Drain to gate isolating spacer. **g** Metallic vias and contact pads

A conventional photolithography process has been developed to enable large-scale manufacturing of Si VNW MOSFETs.

The starting substrate is a 4-in. Si (100) wafer, boron doped at 2×10^{19} atm/cm³, to realize p-type MOSFETs. The Si VNWs are realized based on a top-down approach, through the transfer of hard mask by plasma etching onto the silicon substrate. First, electron beam lithography is used to pattern a high-resolution inorganic resist, hydrogen silsesquioxane (HSQ), in order to fabricate tiny nanopillars with high aspect ratio, up to 7.5, in 150-nm HSQ thickness. A perfectly circular shape with a dispersion of 1.62 nm (1σ) was obtained thanks to an original design—namely a star-like design—which consists of lines starting and finishing in the center of the pattern to force the symmetry of the nanopillars and promote an homogeneous distribution of Gaussian energy [17]. The electron beam exposure is carried out with a Raith 150 system at low energy (20 kV) with a base dose of 300 $\mu\text{C}/\text{cm}^2$ and a current of 120 pA. The revelation of the resist after exposure is performed in tetra methyl hydroxyl ammonium solution at high concentration (25 % in water) to enhance the pattern contrast. The Si VNWs are obtained by performing plasma etching using chlorine chemistry, low pressure (2 mTorr), and 80 W bias power in pure capacitive coupling plasma (CCP) to promote the anisotropy of nanowire sidewalls [18]. VNWs with 94 % of anisotropy are obtained without any visible damage or rugosity on the surface of the NWs. The silicon etching rate is 80 nm/min with a selectivity Si:HSQ = 2:1. The residual resist is stripped in diluted hydrofluoric acid solution. Finally, VNWs are thinned by a sacrificial wet oxidation at 850 °C for 10 min. Thanks to the stress-retarded oxidation effect during the oxide growth [19], the nanowire thinning is controllable [20] and the new interface is free from defects generated by the plasma step. Nanowire networks with maximal yield and reproducibility, without surface roughness or geometrical irregularities, are obtained. In Fig. 2a, a Si VNW network with a 25-nm diameter is presented with an excellent reproducibility.

The gate oxide is realized by dry oxidation at 725 °C over 30 min. The thickness of the grown SiO₂ is around 4 nm and is wrapping the entire VNW's structure.

Before the implementation of platinum silicides (PtSi) for the realization of metallic source/drain contacts, the SiO₂ layer is etched selectively by CCP mode plasma at both sides of the VNWs using a fluorine chemistry (CHF₃:CF₄:Ar = 20:20:10). The source contact is defined by a lift-off process. A 10-nm platinum layer is deposited by electron beam evaporation (anisotropic deposition), followed by the silicide reaction activation using a rapid thermal annealing (RTA) at 500 °C during 3 min under N₂H₂ (96 % 4 %) atmosphere. The VNW sidewalls are cleaned from platinum contaminations by a selective wet etching in aqua regia solution. Figure 2b presents a VNW network with silicided contacts at both sides of the VNWs with clean sidewalls. The 3D process completion must go through a perfect mastery of nanoscale layer engineering. To this end, an innovative planarization method to realize the source to gate isolation spacer was developed using the HSQ as a dielectric material [21]. It is characterized by a low viscosity, providing excellent filling properties. Moreover, the HSQ is a CMOS-compatible material that offers a low dielectric constant ($k \approx 2.7$), minimizing the parasitic capacitances. The planarization process was performed by chemical etching in highly diluted hydrofluoric acid (HF) in deionized water (1:1000). This approach has been preferred to plasma etching or chemical mechanical polishing (CMP); both approaches are widely used to planarize horizontal architectures but are not adapted to 3D architectures. However, the etching of the HSQ in diluted HF needs to take over bubble encroachments on the dielectric surface issued from the releasing of the hydrogen gas during SiO_xH_y etching that induces severe degradations leading to a rough surface. To prevent the bubble encroachment, a cationic surface agent, benzalkonium chloride, has been added to the diluted HF solution. This leads to the extraction of the gas bubbles as they appeared on the surface which then vanish in the solution. The resulting planarization is presented in

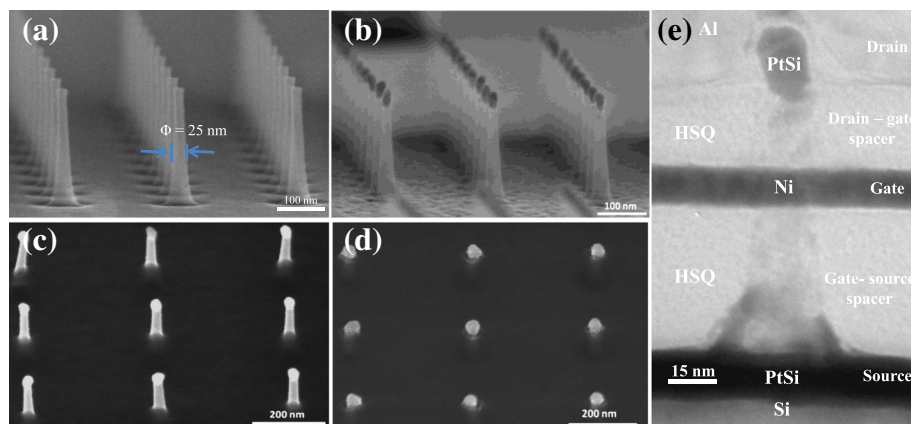


Fig. 2 Tilted SEM images of **a** Si VNW network of 25-nm diameter, **b** PtSi contacts at both side of VNW (**c**) and (**d**), respectively, gate to source and drain to gate insulating spacer formed by HSQ planarization technique and **e** TEM cross-section image of multilayer stacks implemented on VNW arrays

Fig. 2c with a highly planarized HSQ layer over VNWs. It demonstrated an extremely flat layer, minimal roughness below 2 nm (measured by atomic force microscopy), without any degradation of the HSQ surface or of the VNWs. The etching rate of the HSQ is 2.3 nm/s, resulting in a highly controllable process. A 15-nm nickel layer is then

deposited by electron beam evaporation over the gate to source spacer. The gate contact is performed by each back process after the definition of hard mask by photolithography step. The unprotected Ni layer is etched in chemical solution based on $\text{H}_2\text{SO}_4:\text{H}_2\text{O}_2:\text{EDI} = 25:1:50$ ml, followed by the photoresist stripping. For the proposed architecture,

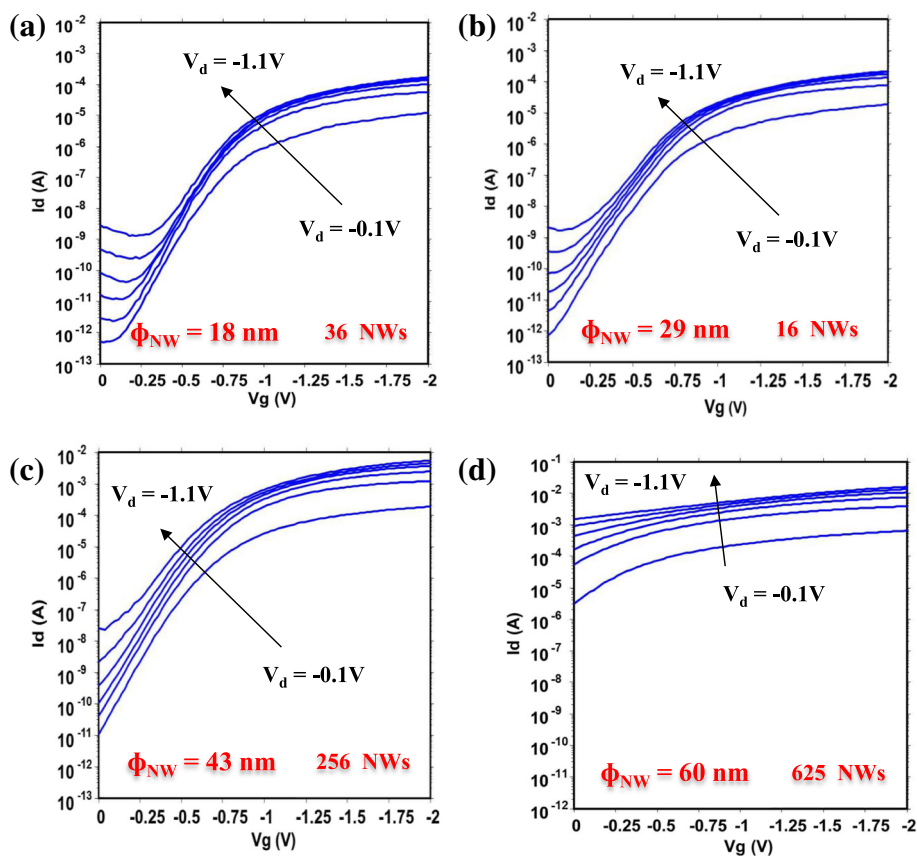


Fig. 3 Transfer characteristics of GAA MOSFET on Si VNW with a diameter of **a** 18 nm, **b** 29 nm, **c** 43 nm, and **d** 60 nm

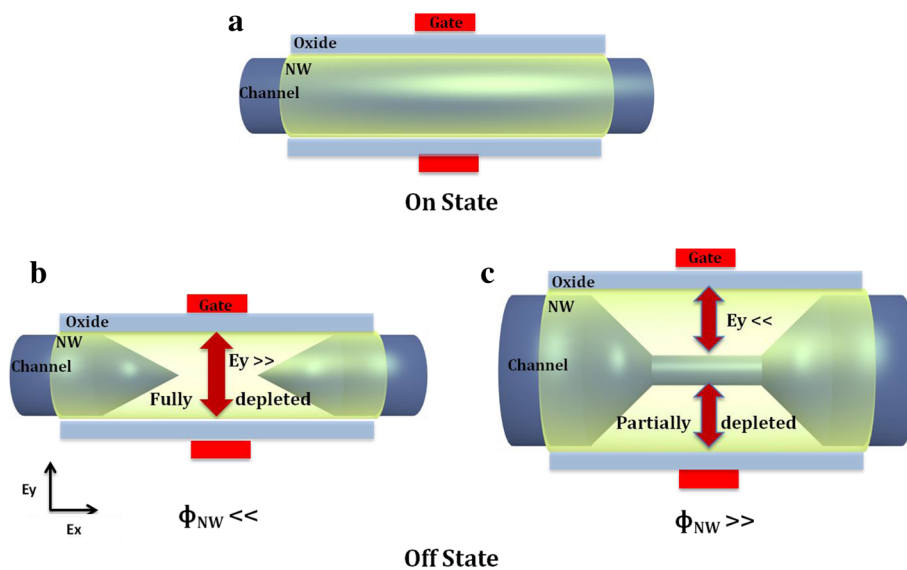


Fig. 4 Schematic representation of the carrier density in the channel at **a** on-state regime and **b, c** off-state regime for thin and large NW diameters, respectively

it is worth noting that the gate length is simply defined by the gate material thickness, without any high-resolution lithography step. A second spacer is then performed to insulate the gate to the drain contacts (Fig. 2d). Via openings are created by plasma etching in the dielectric to contact the metallic source and gate extensions. Finally, a 400-nm thick Al layer is deposited by sputtering followed by a chemical etch back in a solution of $\text{H}_3\text{PO}_4\text{:HNO}_3\text{:EDI} = 5\text{:}40\text{:}7$. Finally, a forming gas anneal (FGA) (N_2H_2 , 96 % 4 %) at 250 °C for 4 min is performed in order to passivate defects at both Si-SiO₂ interface and at Si-PtSi contact interface [22].

Results and discussions

A cross-section image of the device performed by transmission electron microscopy is presented in Fig. 2e and shows the 3D stacking composed of three conductive layers (source, gate, and drain contacts), separated by two insulating layers with homogenous thicknesses and without any defect or damage in the dielectric layers or wave effect at the vicinity of the NWs.

Electrical characterizations of such 3D NW architectures with a nominal gate length of 15 nm have been performed with a Cascade probe and parametric analyzer Agilent 4156C. Static characteristics of devices with different NW diameters (from 18 to 60 nm) are given in Fig. 3. The p-type devices exhibit normally off behavior with high control over short channel effects with almost-ideal subthreshold characteristics ($\text{SS} = 95 \text{ mV/dec}$ and $\text{DIBL} = 25 \text{ mV/V}$) for a device with NW diameter of 18 nm (Fig. 3a). The same characteristics are obtained when the NWs have a diameter of 29 nm (Fig. 3b) and 43 nm (Fig. 3c). The devices exhibit high drive current (normalized by the number and the diameter of NWs) of 431/472 $\mu\text{A}/\mu\text{m}$ when the NW

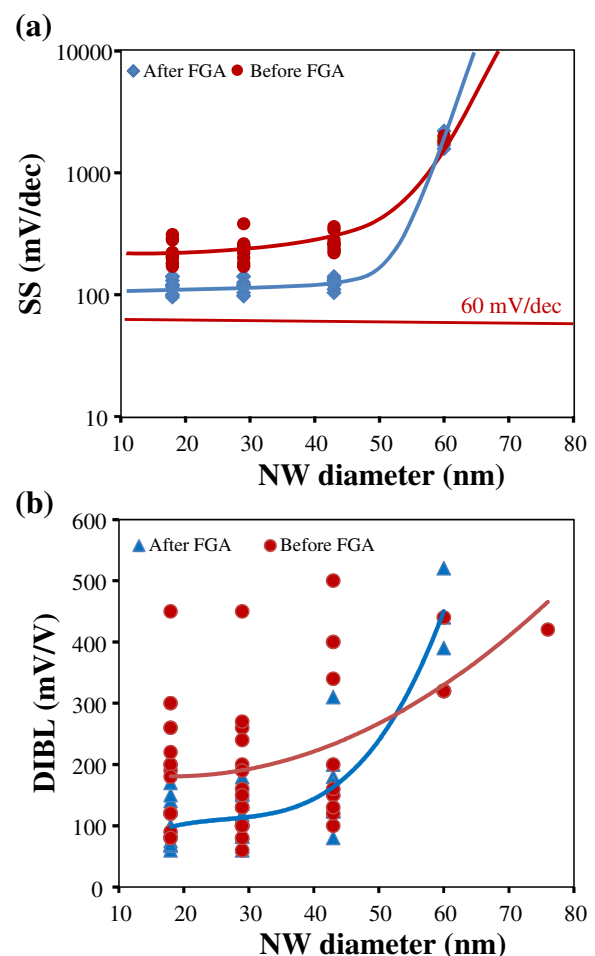
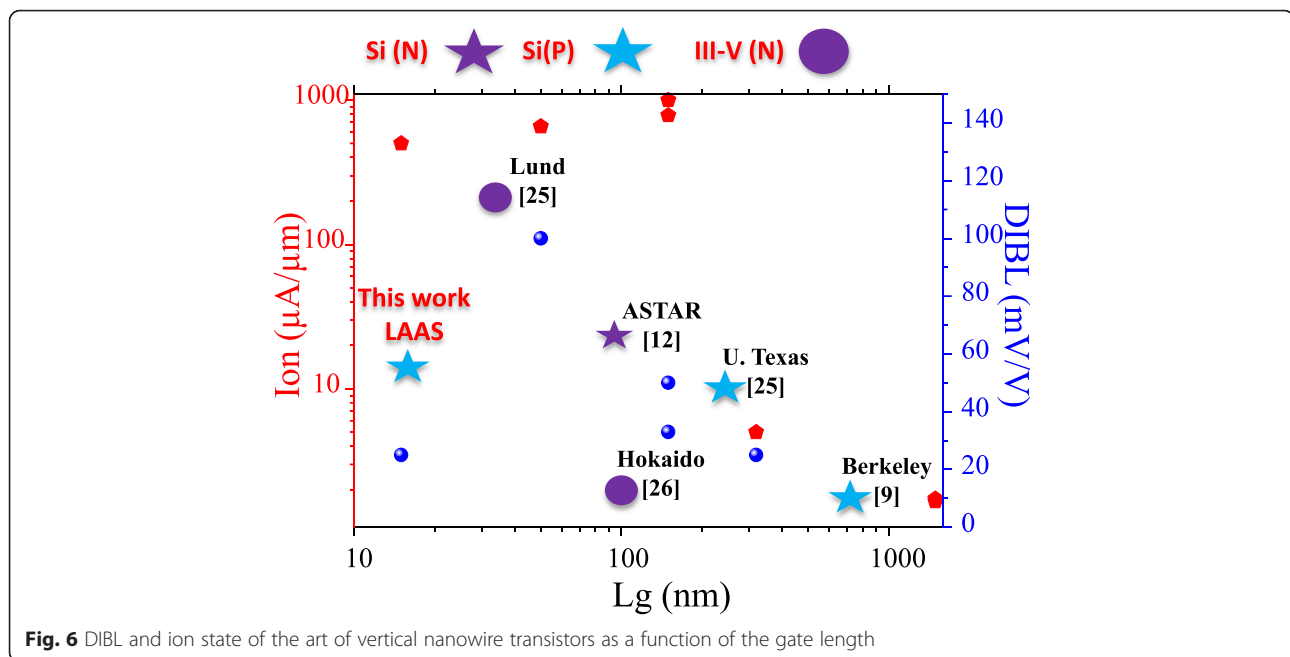


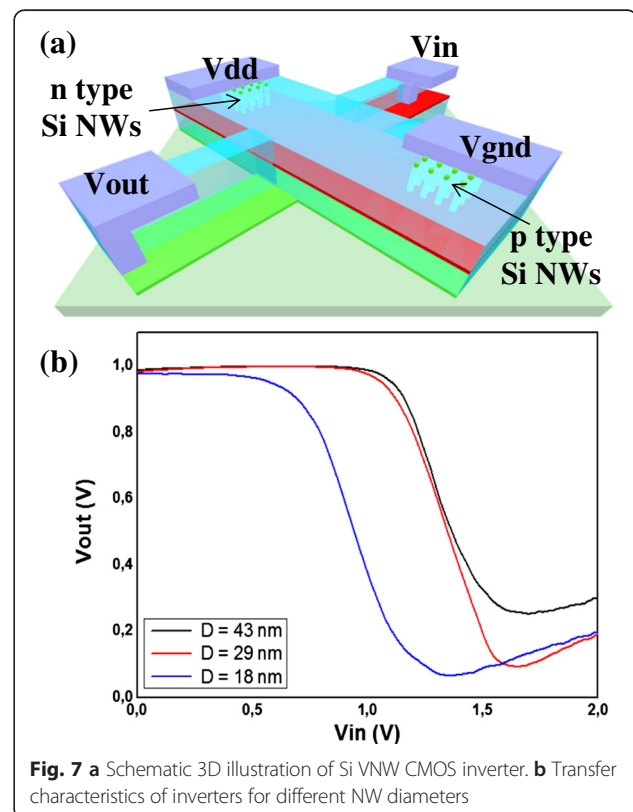
Fig. 5 Impact of forming gas annealing on **a** SS and **b** DIBL as a function of NW diameters



diameters are of 29 nm/43 nm, respectively. When the NW diameter becomes larger than 40 nm (Fig. 3d), the electrostatic control of the gate degrades quickly, and it is no longer able to turn off the device. Figure 4 presents a schematic representation of the carrier density in such a GAA NW configuration in order to explain the impact of the NW diameter on the transistor operation. The device operates in junctionless mode [23] (accumulation mode). When the transistor is turned on (Fig. 4a), the channel conduction is made by the entire section of the NW, which means that the larger the NW diameter is, the larger the drive current per NW is. When the device is turned off, a transverse electrical field (E_y), due to the electrostatic coupling between the gate (metal work function) and the potential in the channel region, induces the depletion of the channel. For narrow diameters (Fig. 4b), the field developed by the gate can deplete the entire volume of the NW. Nevertheless, when the NW is too large (Fig. 4c), the channel is only partially depleted by the gate. A conductive path from the source to the drain is remaining and the transistor cannot be turned off.

Figure 5 summarizes the evolution of the SS (Fig. 5a) and DIBL (Fig. 5b) as a function of NW diameter, before and after the FGA. The defect passivation not only improves the immunity against short channel effects but also greatly reduces device to device variability. Low-frequency noise analysis [24] confirmed the absence of active oxide traps for most wires after the passivation step. Before FGA, the characteristics suffered high variability from device to device, which is supposed to come from the random distribution of interface defects in such miniaturized devices. A comparison to the state of

the art (Fig. 6) of vertical nanowires MOSFET architecture [25–27] frames this result in favorable terms. Even if it is the most scaled demonstration published up to now, the immunity against short channel effect remains robust. Normalized drive current is also high when



compared to p-type transistors. The vertical integration of nanowire transistors is not at the same level of technological maturity as planar/horizontal integration; however, this experimental demonstration shows that this 3D NW architecture should be considered a potential candidate for a sub-5-nm technology node [14].

Finally, in the last section of this report, a first proof of concept for a CMOS inverter based on 15-nm GAA vertical transistors is presented in Fig. 7. Highly doped wells (2×10^{19} atm/cm³) with phosphorous and boron species are performed by conventional ion implantation in order to pattern n- and p-type Si VNWs on the same wafer. A similar transistor process, as described in Fig. 1, is implemented to realize CMOS inverters. Such a 3D architecture is schematically shown in Fig. 7a. The transfer characteristics of inverters implemented on different NW diameters are presented in Fig. 7b, showing regular inverter behavior with sharp commutation from high to low state. Contact engineering for NMOS counterpart is mandatory to enhance the switching characteristics of the inverter by implementing, for example, dopant segregation techniques [28] to reduce the large Schottky barrier to electrons of Pt silicide.

Conclusions

In summary, a large-scale process of Si VNW MOSFETs with nanoscale GAA is presented. The nanowire arrays were made by a top-down approach, and the vertical transistor was realized by a successive engineering of nanoscale thin films using conventional UV lithography. The electrical performances demonstrated excellent electrostatic behavior of the device for a 15-nm gate length, with very good immunity against short channel effects. Finally, a proof of concept for a CMOS inverter by dual integration of n- and p-type Si VNWs was proposed.

Competing interests

The authors declare that they have no competing interests.

Authors' contributions

YG performed the experiments and the electrical characterization. YG and GL discussed the results and wrote the manuscript. GL provided the concept and designed the structures. All authors read and approved the final manuscript.

Acknowledgements

The authors wish to thank F. Cristiano and D. Troadec for TEM analysis. This work was supported by the French RENATECH network (French national nanofabrication platform).

Received: 29 January 2016 Accepted: 4 April 2016

Published online: 19 April 2016

References

1. Appenzeller J, Knoch J, Tutuc E, Reuter M, and Guha S (2006) Dual-gate silicon nanowire transistors with nickel silicide contacts. In: International Electron Devices Meeting. IEDM'06, pp. 1–4.
2. Bangsaruntip S, Cohen GM, Majumdar A, Zhang Y, Engelmann SU, Fuller NCM, Gignac LM, Mittal S, Newbury JS, Guillom M, Barwicz T, Sekaric L, Frank MM, and Sleight JW (2009) High performance and highly uniform gate-all-around silicon nanowire MOSFETs with wire size dependent scaling. Austin, Texas, USA: IEEE International Conference on Integrated Circuit Design and Technology and Tutorial, 2008.ICICDT 2008; p. 1–4.
3. Ernst T, Bernard E, Dupre C, Hubert A, Becu S, Guillaumot B, Rozeau O, Thomas O, Coronel P, Hartmann J-M, Vizioz C, Vulliet N, Faynot O, Skotnicki T and Deleonibus S (2008) 3D multichannels and stacked nanowires technologies for new design opportunities in nanoelectronics. IEEE International Electron Devices Meeting. IEDM'08, San Francisco, California, USA pp. 265–268.
4. Park D (2006) 3 Dimensional GAA transistors: twin silicon nanowire MOSFET and multi-bridge-channel MOSFET. In: 2006 IEEE International SOI Conference., pp 131–134
5. Yeo KH, Suk SD, Li M, Yeoh Y, Cho KH, Hong K-H, Yun S, Lee MS, Cho N, Lee K, Hwang D, Park B, Kim D-W, Park D, Ryu B-I (2006) Gate-all-around (GAA) twin silicon nanowire MOSFET (TSNWFET) with 15 nm length gate and 4 nm radius nanowires. In: Electron Devices Meeting, 2006. IEDM '06. International, pp 1–4
6. Ferain I, Colinge CA, Colinge J-P (2011) Multigate transistors as the future of classical metal-oxide-semiconductor field-effect transistors. *Nature* 479(7373):310–316
7. Lee C-W, Yun S-R-N, Yu C-G, Park J-T, Colinge J-P (2007) Device design guidelines for nano-scale MuGFETs. *Solid-State Electron* 51(3):505–510
8. Ansari L, Feldman B, Fagas G, Colinge J-P, Greer JC (2010) Simulation of junctionless Si nanowire transistors with 3 nm gate length. *Appl Phys Lett* 97(6):062105
9. Goldberger J, Hochbaum AI, Fan R, Yang P (2006) Silicon vertically integrated nanowire field effect transistors. *Nano Lett* 6(5):973–977
10. Singh N, Agarwal A, Bera LK, Liow TY, Yang R, Rustagi SC, Tung CH, Kumar R, Lo GQ, Balasubramanian N, Kwong D-L (2006) High-performance fully depleted silicon nanowire gate-all-around CMOS devices. *IEEE Electron Device Lett* 27(5):383–386
11. Suk SD, Lee S-Y, Kim S-M, Yoon E-J, Kim M-S, Li M, Oh CW, Yeo KH, Kim SH, Shin D-S, Lee K, Park HS, Han JN, Park CJ, Park J-B, Kim D-W, Park D and Ryu B-I (2005) High performance 5nm radius twin silicon nanowire MOSFET (TSNWFET): fabrication on bulk si wafer, characteristics, and reliability. In: IEEE International Electron Devices Meeting, 2005. IEDM Technical Digest. pp. 717–720.
12. Yang B, Buddharaju KD, Teo SHG, Singh N, Lo GQ, Kwong DL (2008) Vertical silicon-nanowire formation and gate-all-around MOSFET. *Electron Device Lett IEEE* 29(7):791–794
13. Kwong D-L, Li X, Sun Y, Ramanathan G, Chen ZX, Wong SM, Li Y, Shen NS, Buddharaju K, Yu YH, Lee SJ, Singh N and Lo GQ (2012) Vertical Silicon Nanowire Platform for Low Power Electronics and Clean Energy Applications. *J. Nanotechnol article ID 492121*, 2012:21 doi:10.1155/2012/492121
14. Thean AV-Y, Yakimets D, Huynh Bao T, Shuddindin P, Sakhare S, Garcia Bardon M, Sibaja-Hernandez A, Ciofi I, Eneman G, Veloso A, Ryckaert J, Raghavan P, Mercha A, Mocuta A, Tokei Z, Verkest D, Wambacq P, De Meyer K, Collaert N (2015) Vertical device architecture for 5nm and beyond: device & circuit implications. Symposium on VLSI Technology Digest of Technical Papers, pp 27–28
15. Larrieu G, Han X-L (2013) Vertical nanowire array-based field effect transistors for ultimate scaling. *Nanoscale* 5(6):2437
16. Larrieu G, Guerfi Y, Han XL, Clement N (2015) Vertical field effect transistor with sub-15 nm gate-all-around on Si nanowire array. In: Solid State Device Research Conference (ESSDERC), 2015 45th European., pp 202–205
17. Guerfi Y, Carcenac F, Larrieu G (2013) High resolution HSQ nanopillar arrays with low energy electron beam lithography. *Microelectron Eng* 110:173–176
18. Han XL, Larrieu G, Dubois E (2010) Realization of vertical silicon nanowire networks with an ultra-high density by top-down approach. *J Nanosci Nanotechnol* 10:7423–7427
19. Rzeminski C, Han XL, Larrieu G (2012) Understanding of the retarded oxidation effects in silicon nanostructures. *Appl Phys Lett* 100:26, 263111–1–4
20. Han XL, Larrieu G, Fazzini PF, Dubois E (2011) Realization of ultra-dense arrays of vertical silicon NWs with defect free surface and perfect anisotropy using a top-down approach. *Microelectron Eng* 88(8):2622–2624
21. Guerfi Y, Doucet J-B, Larrieu G (2015) Thin-dielectric-layer engineering for 3D nanostructure integration using an innovative planarization approach. *Nanotechnology* 26:425302
22. Han XL, Larrieu G, Dubois E, Cristiano F (2012) Carrier injection at silicide/silicon interfaces in nanowire based-nanocontacts. *Surf Sci* 606(9–10):836–839

23. Colinge J-P, Chi-Woo Lee C, Afzalian A, Akhavan N, Yan Y, Ferain I, Razavi P, O'Neill B, Blake A, White M, Kelleher A, McCarthy B, Murphy R (2010) Nanowire transistors without junctions. *Nat Nanotechnol* 5:225–229
24. Clement N, Han XL, Larrieu G (2013) *Appl Phys Lett* 103:263504
25. Zhai Y, Mathew L, Rao R, Palard M, Chopra S, Ekerdt JG, Register LF, Banerjee SK (2014) High-performance vertical gate-all-around silicon nanowire FET with high-k/metal gate. *IEEE Trans Electron Devices* 61(11):3896–3900
26. Tomioka K, Yoshimura M, Fukui T (2012) A III–V nanowire channel on silicon for high-performance vertical transistors. *Nature* 488(7410):189–192
27. Thelander C, FrobergFroberg LE, Rehnstedt C, Samuelson L, Wernersson L-E (2008) Vertical enhancement-mode InAs nanowire field-effect transistor with 50-nm wrap gate. *IEEE Electron Device Lett* 29(3):206–208
28. Larrieu G, Dubois E (2011) CMOS inverter based on Schottky source-drain MOS technology with low temperature dopant segregation. *IEEE Electron Device Lett* 32(6):728–730

Submit your manuscript to a SpringerOpen[®] journal and benefit from:

- Convenient online submission
- Rigorous peer review
- Immediate publication on acceptance
- Open access: articles freely available online
- High visibility within the field
- Retaining the copyright to your article

Submit your next manuscript at ► springeropen.com
